ORCA – Online Research @ Cardiff

Electrochemical Sensing of Ascorbic Acid, Hydrogen Peroxide and Glucose by Bimetallic (Fe, Ni)-CNTs Composite Modified Electrode

Sayed Tayyab Raza Naqvi,[a] Bahareh Shirinfar,[b] Dilshad Hussain,[a,c] Saadat Majeed,[a]* Muhammad Naeem Ashiq,[a] Yasin Aslam[a] and Nisar Ahmed[b,c,d]*

[a]Division of Analytical Chemistry, Institute of Chemical Sciences, Bahauddin Zakariya University, Multan 60800, Pakistan

[b]School of Chemistry, University of Bristol, Bristol, BS8 1TS, United Kingdom.

[c]International Centre for Chemical and Biological Sciences, HEJ Research Institute of Chemistry, University of Karachi, Karachi 75270, Pakistan

[d]School of Chemistry, Cardiff University, Main Building, Park Place, Cardiff, CF10 3A, United Kingdom.

*E-mail:saadat.majeed@bzu.edu.pk (SM), AhmedN14@cardiff.ac.uk (NA)

Abstract

In this research, bimetallic supported CNT modified electrode (Fe,Ni/CNTs/GCE) has been developed for sensitive, stable and highly elctroactive sensing of glucose, ascorbic acid and hydrogen peroxide. Transition metals such as Iron (Fe) and Nickel (Ni) offer high electrical and thermal conductance, high active surface-to-volume ratio and presence of d-band electrons gives enhanced electrocatalytic behavior. While, CNTs provide high surface area, stability and excellent conductivity. Synthesized material is characterized by SEM, EDS, XRD and FTIR to access morphology, elemental composition and structure. This unique combination is employed for the electrochemical sensing of ascorbic acid, glucose and hydrogen peroxide and different experimental parameters are optimized. Fe,Ni/CNTs/GCE shows good sensing efficiency at pH 7.4 which is ideally suitable for variety of analytes. The modified electrode also show good reproducibility and sensitivity under optimized conditions and can be reused upto 30 cycles without compromising the efficiency. With good linearity, reproducibility and limit of detection, this material possess significant potential as non-enzymatic biosensor for variety of analytes.

Key Words: Bimetallic nanocomposite, Carbon nanotubes, Ascorbic acid, Glucose, Hydrogen peroxide, Electrochemical sensing

1   Introduction

Ascorbic acid, glucose and hydrogen peroxide are important biological compounds. Ascorbic acid, commonly known as Vitamin C, improves the immune system due to its unique antioxidant properties. It also protects against cancer and retina muscular degeneration [1]. Ascorbic acid also aids the body to produce collagen which is an important constituent of the connective tissues, gums, blood vessels and bones. Furthermore, it facilitates the recovery of tissues after surgery and different type of wounds [2]. Ascorbic acid deficiency may cause Scurvy, a disease in which patient suffers to swollen gums, muscle weakness, bleeding under the skin layer, bleeding through gums, depression and tiredness and loss of teeth [3]. Abundance of ascorbic acid in human tissues can cause breakdown of alcohol and its high dose may lead to kidney stones, nausea, vitamin B12 deficiencies, diarrhea, increased need for oxygen and copper deficiencies [4].

Similarly, glucose is the main energy source in living organisms and it is a very common fuel in biological system, especially used in muscles and brain[5]. In most organisms, from bacteria to humus, it provides energy through fermentation, aerobic respiration and anaerobic respiration [6] and approximately3.75 kilocalories of energy can be attained per gram with the aid of aerobic respiration [7]. Although glucose provides energy but overdose is problematic especially for diabetic patients. High sugar level can lead to tooth decay and health problem, weight gain and diabetes [8]. Animals store glucose in the form of glycogen and plants store glucose in the form of starch which provides immunity against parasites and insecticides as well as for cancerous cells [9]. These cells usually do not have mechanism to break down the hydrogen peroxide thus they act as proved anti-cancer agents [10]. Excessive level of hydrogen peroxide with normal endogenous level of antioxidant enzyme cause oxidative stress in brain and

cause apoptosis and cell tissue damage. Due to its oxidative stress in human body fluids and metabolism it may cause diabetes mellitus, cancer and hepatic diseases [11].

Therefore it is very important to design sensitive, easy, accurate and point of care sensing devices for sensing and detection of glucose, hydrogen peroxide and ascorbic acid in clinical treatment and diagnosis. In past decade, variety of techniques has been involved in sensing of redox active biological molecules including spectrophotometry, immunoassay, fluorescence colorimetry, chemiluminescence and electrochemical techniques [12]. Among these techniques, electrochemical detection and sensing differentiate itself due to less complexity, rapid response, user-friendliness and low cost [13]. Conventionally, electrochemical sensors have been developed by immobilizing enzyme on electroactive species [14]. In spite of providing high sensitivity and selectivity, enzymatic electrochemical sensors suffer from several disadvantages such as difficult purification of enzyme, less environmental stability, laborious immobilization, loss of enzyme activity during immobilization, denaturation, high cost and time consuming [15].

As solution, non-enzymatic electrochemical sensors have been developed as an alternative to enzymatic electrochemical sensors [16]. These non-enzymatic electrochemical sensors are based on various nanofabricated materials owing to their inherent catalytic behavior towards electrochemically active biological molecules, low cost and non-laborious development, and their operative ease and long lasting stability [17]. Different types of non-enzymatic electrochemical sensors have been developed including gels [18], conductive polymers [19], nanoparticles and nanocomposites of transition metals [20], fabricated metal organic framework [21], and carbon based materials [22].

Metals and their composites, due to their specific electronic arrangement shows high electrical and thermal conductance, high active surface-to-volume ratio and presence of d-band

electrons give enhanced electrocatalytic behavior [23], have been vastly employed in development of non-enzymatic electrochemical transducers for sensing of biomolecules [24]. These types of sensors face disadvantages of reduced selectivity and sensitivity, high price and disappearance of activity due to deposition of intermediate compounds and chloride ion. On the other hand, with notable progress in synthesis of modified nanomaterials for electro-catalysis, various non-metallic nanomaterials have also been utilized [25]. For modified electro-catalyst nanomaterials, various supporting materials like graphene, carbon nanotubes, nanofoams and polymers, showing good conductance and stability, have been used to develop modified electro-catalyst and electrochemical sensing of biomolecules [26]. These modified electro-catalyst also experience certain drawback during development such as the addition of supporting material block many active sites on catalyst, resulting small number of active sites involve in electro-catalysis. So transition metal based electrochemical sensors, like Ni, Fe, Cu, Co, and Mn based nanomaterials, have attracted the interest of researchers in recent years [27]. Composites of metals with other metals, with polymers and carbon based materials have often resulted in superior performance of the sensing material because each part of the composite plays its role in sensing [28]. These materials, in composite form, have higher surface area, provide multiple active sites for the attachment of target molecule and offer unique chemistry to improve the sensitivity and selectivity of biomolecules [29].

In this research work, bimetallic supported carbon nanotubes (CNTs) modified electrode (Fe,Ni/CNTs/GCE) has been developed for fast and sensitive detection of glucose, ascorbic acid and hydrogen per oxide. CNTs have been used due to their enhanced surface area, high stability and excellent conductivity. In order to achieve combined electrochemical activities of both metals, Nickel and Iron, bimetallic nanoparticles have been synthesized by co-precipitation

method. These bimetallic nanoparticles have been supported on CNT modified electrode (Fe,Ni/CNTs/GCE) for electrochemical studies of three biologically important molecules.

2 Experimental Section

2.1 Chemicals and Reagents

All reagents and chemicals used in this work were of analytical grade and used without any further purification. $NiCl_2.6H_2O$ (Sigma Aldrich), $FeSO_4.7H_2O$ (Sigma Aldrich), NaOH(Anal R), Sodium borohydride (Anal R), Deionized water, Acetone (Sigma Aldrich), Ethanol (Merck), Glucose (KANTO Chemical CO.), Hydrogen peroxide (KANTO Chemical CO.), Ascorbic acid (Anal R), potassium Dihydrogen phosphate (KANTO Chemical CO.), Dipotassium hydrogen phosphate (Merck), Carbon nanotubes (Merck) , Methyl silicone oil (Sigma Aldrich).

2.2 Synthesis of Bimetallic (Ni, Fe) Nanocomposites

12.3 g of $FeSO_4.7H_2O$ [44 mmol] and 3.0 g of $NiCl_2.6H_2O$ [12.6 mmol] were dissolved in 100 mL deionized water and stirred for 10 minutes. Then pH of the solution was maintained at 7 by using 0.1M NaOH. The solution was taken two neck flask and 6g sodium borohydride was added to the reaction mixture which act as reducing agent and stirred at 60 ℃ for 30 minutes. After 30 minutes precipitates were formed which were separated by filtration. The precipitates were washed thrice with distilled water and acetone, respectively and dried in oven at 100 ℃ for three hours. The precipitates were grinded to a fine powder and stored in desiccator prior to further use [30].

2.3 Instrumentation and Characterization Techniques

FTIR was performed for functional group determination of sample. Crystal structure was determined by X-Ray diffraction (XRD, advance diffractometer). SEM and EDS analysis was performed for morphology and elemental composition of bimetallic composite. All the

electrochemical experiments were performed by using the AutoLab (Potentiostat) in Bahauddin Zakariya University Multan and Quaid-e-Azam, University, Islamabad.

2.4   Electrochemical Measurements

For standardization of modified electrode a solution of potassium ferrocyanide $[K_4(CN)_6Fe]$ of known concentration was prepared. For this purpose, 0.04 g of 1mM solution of potassium ferrocyanide and 7.4 g of 0.1M potassium chloride were dissolved in 100 mL of deionized water. Electrode was prepared to check its redox behavior in potassium ferrocyanide solution. The electrodes were washed thrice first with detergent, ethanol and followed by distilled water, sonicated for 15 minutes, and dried in oven. 2 mg of sample and 4mg of carbon nano tubes (CNTs) were mixed and grounded with the help of pestle and mortar. 50 µL of methyl silicone oil was added to the mixture as binder. Thick slurry was formed and this slurry was further used to fill the glassy carbon electrode by using micro spatula. The electrode surface was cleaned regularly before every run of sample.

The solutions of different concentration of glucose, hydrogen peroxide, and ascorbic acid were prepared in phosphate buffer solution. The oxidation and reduction behavior of glucose, ascorbic acid and hydrogen peroxide was observed by cyclic voltammetry at optimized conditions of pH, scan rate and concentration.Three electrode system consisting of a working electrode (glassy carbon electrode), standard electrode (platinum wire) and counter electrode (silver/silver chloride) was used for all the electrochemical measurements.

3   Results and Discussion

3.1   Characterization of Material

For characterization of bimetallic composite ATR analysis is carried out and ATR spectra of bimetallic nanoparticles is given in Fig. S1 (supporting Information). Presence of distinct band at

3349 cm^{-1} indicate OH bond which is present on the surface of metal oxides and metal oxide composites. Peak appeared at 1347 cm^{-1} is due to the stretching vibration of the C-O group. Peaks present in fingerprint region (767 and 745 cm^{-1}) indicate the presence of metal oxide bond which is attributed to longitudinal vibrations. The Ni-O and Fe-O bonds vibrations can contribute to the spectral region of low wavenumbers (less than 800 cm^{-1}) and the supported oxide can give rise to new sites with different chemical environments (Ni-O-Fe). The XRD patterns of bimetallic nanocomposites are given in Fig. S2 (Supporting Information). Peak at 48^0 is observed for Ni nanoparticles which are diffraction peaks related to the cubic structure. The diffraction peak at 2Θ 39.6^0 and 82.7^0 related to crystal plane diffraction peaks of a-Fe$_2$O$_3$ (JCPDS #33-0664) respectively for bimetallic nanoparticles. Moreover, SEM and EDS analysis is carried out to access the morphology, particle size of the bimetallic composite and elemental composition of the prepared nanocomposites. Fig. S3A and S3B shows the SEM image and EDX graph of the material. Composite material has irregular morphology and particle size is around 80 to 100 nm. On the other hand, all the constituents of the composite material are present in appropriate ratio (Fig. S3B).

3.2   Sensing of Ascorbic Acid by Fe, Ni/CNTs/GCE

Figure 1 shows electrochemical redox behavior of Fe,Ni/CNTs/GCE and bare GCE in potassium ferrocyanide solution. No obvious peak (red) observed at bare glassy carbon electrode, indicating no electrocatalytic behavior. However, at Fe,Ni/CNTs/ GCE two well defined oxidation and reduction peaks (black) are observed at +0.8V and 0.4 V (vs Ag/AgCl), respectively. The result indicates that as prepared electrode good redox behavior and can be use further for analysis of analytes.
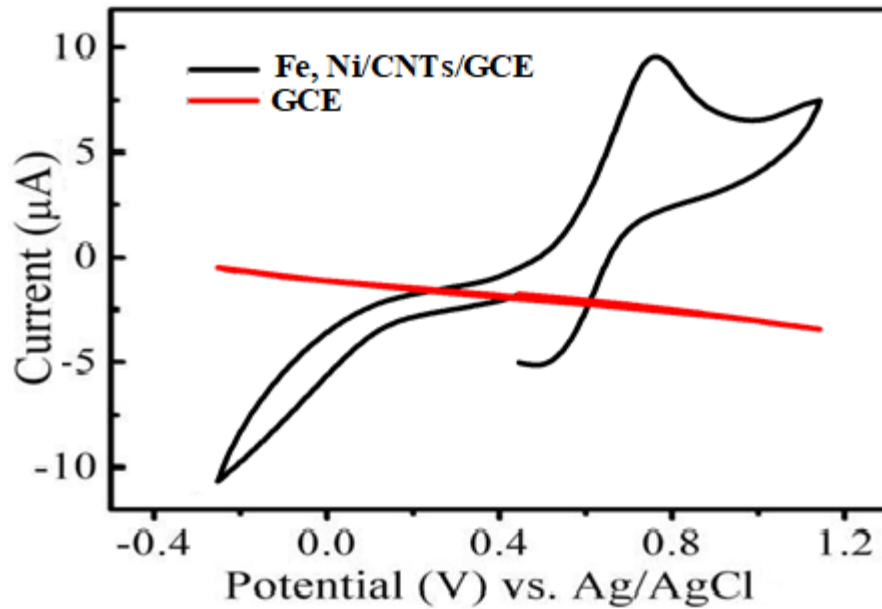
Fig. 1. CV curves for Fe, Ni/CNTs/GCE (black) and bare GCE (red) in potassium ferrocyanide solution.

Then material is applied for sensing of ascorbic acid. Fig. 2A shows the oxidation and reduction peaks at various concentrations (1mM, 10mM, 15mM, 30mM and 40mM) of ascorbic acid which are prepared in PBS of pH 7.4 and analyzed in a potential window of 0.0V to +1.0V. A blank solution is also run on cyclic voltammetry, and no oxidation reduction peak is observed in that solution. With increasing the concentration of analyte (ascorbic acid) current also increased linearly at +0.6V potential. The maximum oxidation current is observed for 40mM solution. These results show that Fe, Ni/CNTs/ GCE possess significant potential for sensing of ascorbic acid. A graph is plotted between concentration of analyte and the current produced. Fig. 2B shows the linear graph indicating a direct relationship between the current and the concentration of ascorbic acid. The current produced at different concentration is taken from the oxidation peaks. The electrode contain linear dependence (y = mx+c) and R^2 in the range of

0.995, limit of detection was 3.60 µM and the relative standard deviation was 4.98%. The results indicate the good sensing ability and highly sensitive behavior of prepared material for ascorbic acid.
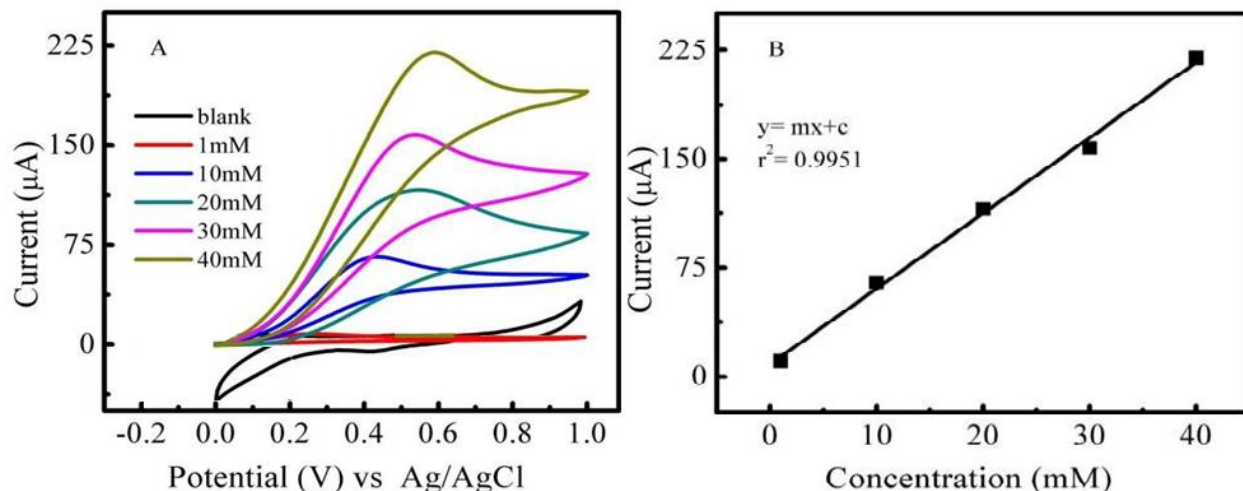

Fig. 2. CV curves (A) and linear plot (B) for concentration optimization of ascorbic acid at Fe,Ni/CNTs/GCE. Conditions: Scan rate 0.5V/s, potential 0.0V to +1.0V, concentration of ascorbic acid; blank (0mM), 1, 10, 20, 30, 40 mM), pH 7 PBS. (N=3, 90% confidence limit).

3.3 Sensing of Glucose on Modified Fe, Ni/CNTs/GCE

Then material is also tested for the electrochemical sensing of glucose. Fig. 3A shows the redox behavior of glucose in different lower concentrations ranging from 1mM to 20 mM solution in PBS (pH 7.4). It is obvious from the graph that when concentration of the glucose increases the current also increase. Highest current is observed for 20 mM solution and lowest for 1mM. Fig. 3B shows the good linear correlation between the concentration of glucose and the current indicating a direct relationship between the two parameters. For glucose, the modified electrode contain linear dependence of $R^2 = 0.661$. The limit of detection and relative standard deviation are also calculated which are 16.89 µM and 13.57%, respectively. With further increase in

concentration to higher value from 40 mM to 90 mM, the current intensity increased constantly (Fig. S4A). Fig. S4B shows the good linear correlation between the concentration and the current with linear dependence for R^2 = 0.96. The limit of detection and relative standard deviation is also calculated which are 1.23 µM and 4.85%, respectively. These results indicate that detection is more accurate at higher concentration and linearity is also improved significantly.
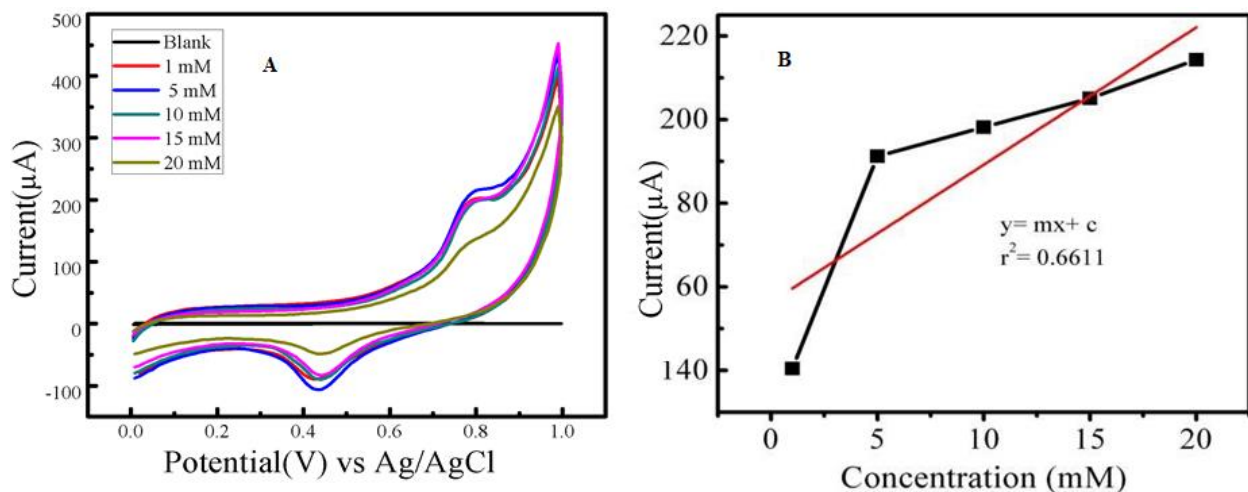

Fig. 3. CV curves (A) and linear plot (B) for optimization of concentration of glucose at Fe,Ni/CNTs/GCE. Conditions: Scan rate 50 mV/sec, potential of the window 0.0V to 1.0V, lower concentration range of glucose, blank (0mM) and 1, 5, 10, 15 and 20 mM, pH 7.4 PBS.

Furthermore, scan rate is also optimized to access the best possible redox conditions. Fig. 4A shows the cyclic voltammogram of glucose at different scan rates (from 10mV/s to 50mV/s). It is observed that with increasing the scan rate from 10mV/s to 50mV/s there is a constant increase in the current. The maximum current is observed at 50mV/s scan rate and minimum current is for 10mV/s. There is direct relation between scan rate and current as the scan rate

increased the current also increased. Moreover, Fig. 4B shows the correlation between the potential and current at different scan rates. There is a direct relationship between current and potential for the current produced due to oxidation and reduction at different scan rates. Maximum oxidation current and minimum reduction current is observed at 50mV/s scan rate while maximum reduction current and minimum oxidation current is observed at 10mV/s. Therefore, graph shows two straight lines for anodic and oxidative current respectively. R^2 value for oxidation and reduction are 0.97 and 0.99, respectively.
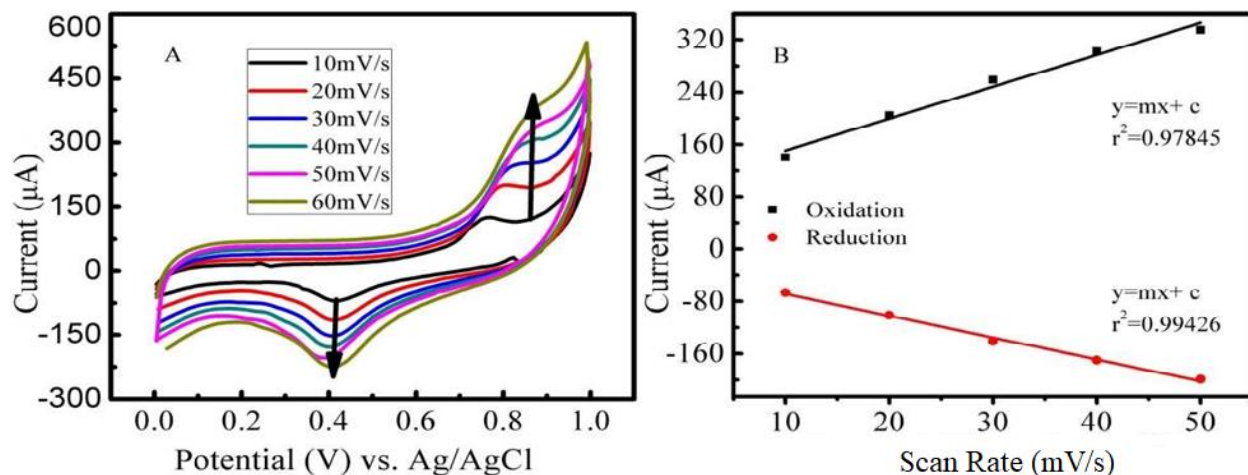

Fig. 4. CV curve for scan rate effect (A) and linear plot (B) for glucose at Fe, Ni/CNTs/GCE. Conditions: potential window 0.0V to 1.0V, glucose 10mM, pH 7.4 PBS.Scan rate 10,20,30,40,50 mV/s, (N=3, 95% confidence limit). All other conditions are same.

Stability of the electrode is accessed on glucose for 30 cycles. Fig. 5 shows the electrode stability for glucose acquired between the potential (on x-axis) versus current (y-axis). This stability is achieved by repeating the redox behavior thirty times using 10 mM glucose solution in PBS, pH 7.4. After thirty cycles, it is observed that both oxidation and reduction peak curves are obtained at +0.8V and +0.4V, respectively. This indicate excellent stability of

Fe,Ni/CNTs/GCE, upto thirty cycles without any significant change. So, it can be reused several times without compromising the efficiency, showing good reproducibility and cost-effectiveness of the material.
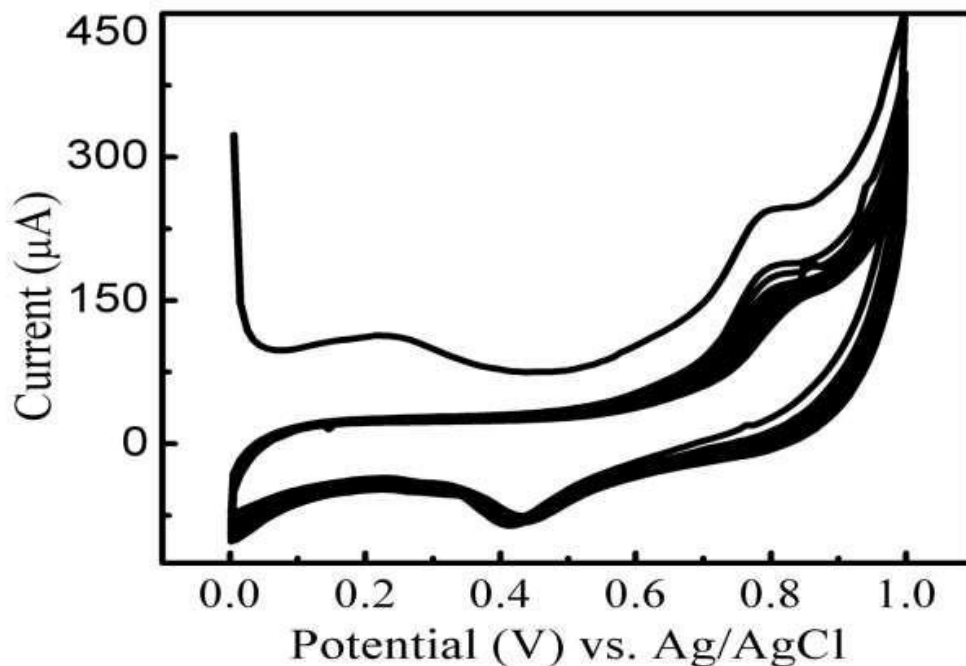

Fig. 5. Stability and reproducibility of Fe, Ni/CNTs/GCE for glucose sensing at the ratio of (1:2) up to 30 cycles. Glucose 10mM, scan rate 50 mV/sec, potential window 0.0 to +1.0V, pH 7.4 PBS.

3.4 Sensing of Hydrogen Peroxide on Fe,Ni/CNTs/GCE

Finally, sensing ability of Fe,Ni/CNTs/GCE is evaluated on hydrogen peroxide. Different concentration solution of hydrogen peroxide is prepared at different pH in order to check the pH effect on sensing of hydrogen peroxide. Very small oxidation and reduction peaks are observed at pH: 10 (Fig. S5, Supporting Information). The best oxidation and reductions trend is observed at pH 7 and clear peaks are observed at pH 7. So, 7.4 pH of phosphate buffer solution is selected

as optimized pH for further experiments. Cyclic voltammogram between pH and current shows that the maximum cathodic current is observed at pH 7.4 but with increasing the pH resulted decrease in current (Figure S6). It suggests that, pH 7.4 is optimum pH for sensing of hydrogen peroxide. Hydrogen peroxide is quite stable at pH 7.4, its degradation is also very low upto pH 10. At very high pH (11, 12), decomposition is very high which can interfere the results due to the production of oxygen. We tested the material at different pH and results indicate that sensing efficiency of bimetallic electrode is best at pH 7.4 at which decomposition is negligible. With increase in pH, the produced current decreases. This might be due to the degradation of hydrogen peroxide and oxygen production, as a result of degradation.

Then concentration of hydrogen peroxide is also optimized (Fig. 6A). The voltammogram shows the oxidation and reduction peaks of various concentration of hydrogen peroxide in a potential window of 0.0V to 0.8V. A blank solution is also run on cyclic voltammetry and no peak is observed. Different concentrations (1mM, 5mM, 10mM and 15mM) are analyzed on cyclic voltammetry using Fe, Ni/CNTs/GCE. Similar trend is observed in this case also, with increasing the concentration of analyte (hydrogen peroxide) the amount of current also increased and maximum oxidation current is observed for 15 mM solution. The graph shows the linear relationship of hydrogen peroxide concentration from 1mM, 5mM, 10mM and 15mM versus current (Fig. 6B) with linear dependence (R^2) 0.9571. Limit of detection and relative standard deviation are 16.89µM and 13.57%, respectively.
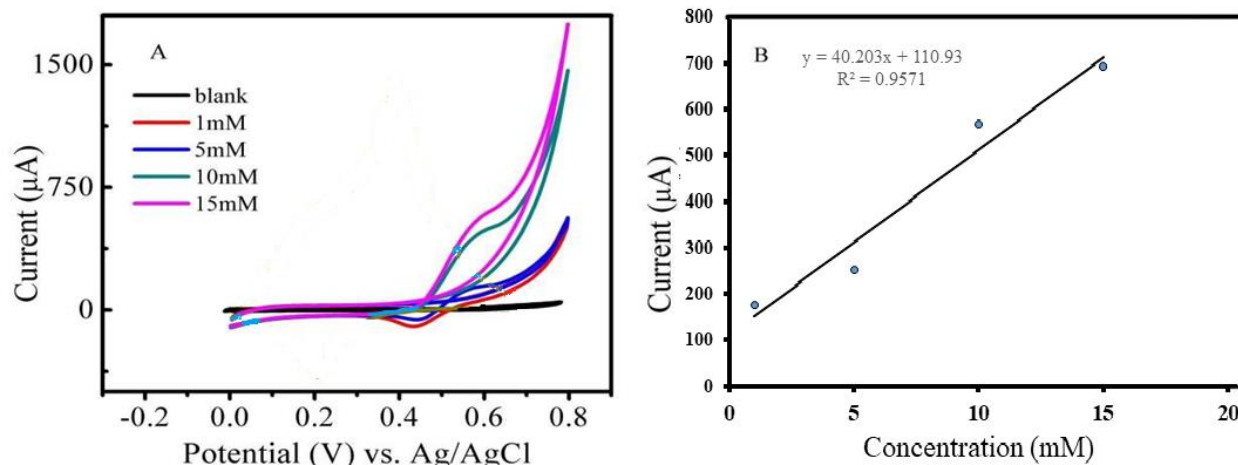
Fig. 6. CV curves (A) and linear plot (B) for concentration optimization of hydrogen peroxide at Fe,Ni/CNTs/GCE. Conditions: Scan rate 50mV/s, potential of the window 0.0V to 0.8V, hydrogen peroxide (1mM, 5mM, 10mM and 15mM), pH 7.4 PBS. (N=3, 90% confidence limit)

4   Conclusion

In this work we prepared a sensing material based on bimetallic (Fe, Ni)-CNTs composite by co-precipitation method and the prepared material is successfully characterized with different techniques including SEM, EDX, FTIR and XRD. This bimetallic composite is used for the sensing of various redox active species (hydrogen peroxide, glucose and ascorbic acid) which are important biomolecules. To maintain their level in biological fluids is very important and any increase or decrease of these molecules could lead to various diseases. The prepared material show a sensitive and reproducible electrochemical sensing of various redox active species and showed good detection limit for ascorbic acid, hydrogen peroxide and glucose. Materials showed excellent reproducibility and stability upto 30 cycles, with compromising the sensing efficiency. All the molecules tested in this study have distinct oxidation potential value and Fe,Ni/CNTs/GCE has the ability to sense these molecules in a very low concentration. And we

assume that under optimized conditions (scan rate, pH and concentration), this material has the potential to distinguish between the molecules with very close oxidation potentials. With further optimization, this material can be used for variety of other biologically important analytes also with good accuracy and sensitivity.

Conflict of interest

Authors describe no conflict of interest in this work.

Conflict of interest

Authors describe no conflict of interest in this work.

References

[1]   A. C. Carr, S. Maggini, *Nutrients* **2017**, *9*, 1211.
[2]   J. M. Pullar, A. C. Carr, M. C. M. Vissers, *Nutrients* **2017**, *9*, 866.
[3]   M. Conway, P. Marcon, P. Meinert, C. Durno, J. E. Upton, M. Kirby-Allen, M. Weinstein, *Pediatrics* **2018**, e20172971.
[4]   J. Du, J. J. Cullen, G. R. Buettner, *Biochimica et Biophysica Acta (BBA)-Reviews on Cancer* **2012**, *1826*, 443-457.
[5]   K. Selvarani, S. Berchmans, *Journal of The Electrochemical Society* **2017**, *164*, H561-H571.
[6]   aR. J. Seeley, S. C. Woods, *Nature Reviews Neuroscience* **2003**, *4*, 901; bW. Gao, W. W. Tjiu, J. Wei, T. Liu, *Talanta* **2014**, *120*, 484-490.
[7]   P. Schönfeld, L. Wojtczak, *Journal of Lipid Research* **2016**, *57*, 943-954.
[8]   P. Moynihan, Y. Makino, P. E. Petersen, H. Ogawa, *Community dentistry and oral epidemiology* **2018**, *46*, 1-7.
[9]   H. van Tong, P. J. Brindley, C. G. Meyer, T. P. Velavan, *EBioMedicine* **2017**, *15*, 12-23.
[10]   O. M. Ighodaro, O. A. Akinloye, *Alexandria Journal of Medicine* **2017**.
[11]   A. Bhattacharyya, R. Chattopadhyay, S. Mitra, S. E. Crowe, *Physiological Reviews* **2014**, *94*, 329-354.
[12]   aM. P. Landry, H. Ando, A. Y. Chen, J. Cao, V. I. Kottadiel, L. Chio, D. Yang, J. Dong, T. K. Lu, M. S. Strano, *Nature Nanotechnology* **2017**, *12*, 368; bZ. Li, J. R. Askim, K. S. Suslick, *Chemical Reviews* **2018**; cD. Fan, C. Shang, W. Gu, E. Wang, S. Dong, *ACS Applied Materials & Interfaces* **2017**, *9*, 25870-25877; dW. Chen, Y. Chen, M. Wang, Y. Chi, *Analyst* **2018**, *143*, 1575-1582.
[13]   aJ.-S. Ye, C.-W. Chen, C.-L. Lee, *Sensors and Actuators B: Chemical* **2015**, *208*, 569-574; bS. T. R. Naqvi, S. Majeed, M. Najam-ul-Haq, D. Hussain, T. Iqbal, N. Ahmed, *Analyst* **2018**.
[14]   S. M. Oja, B. Feldman, M. W. Eshoo, *Analytical Chemistry* **2018**, *90*, 1536-1541.
[15]   X. Chen, G. Wu, Z. Cai, M. Oyama, X. Chen, *Microchimica Acta* **2014**, *181*, 689-705.
[16]   J. He, J. Sunarso, Y. Zhu, Y. Zhong, J. Miao, W. Zhou, Z. Shao, *Sensors and Actuators B: Chemical* **2017**, *244*, 482-491.
[17]   A. A. Ensafi, N. Zandi-Atashbar, B. Rezaei, M. Ghiaci, M. Taghizadeh, *Electrochimica Acta* **2016**, *214*, 208-216.
[18]   S. H. Cho, S. W. Lee, S. Yu, H. Kim, S. Chang, D. Kang, I. Hwang, H. S. Kang, B. Jeong, E. H. Kim, S. M. Cho, K. L. Kim, H. Lee, W. Shim, C. Park, *ACS Applied Materials & Interfaces* **2017**, *9*, 10128-10135.
[19]   G. Wang, A. Morrin, M. Li, N. Liu, X. Luo, *Journal of Materials Chemistry B* **2018**, *6*, 4173-4190.
[20]   Y. Li, Y. Zhong, Y. Zhang, W. Weng, S. Li, *Sensors and Actuators B: Chemical* **2015**, *206*, 735-743.
[21]   M.-Q. Wang, Y. Zhang, S.-J. Bao, Y.-N. Yu, C. Ye, *Electrochimica Acta* **2016**, *190*, 365-370.
[22]   C. Yang, M. E. Denno, P. Pyakurel, B. J. Venton, *Analytica chimica acta* **2015**, *887*, 17-37.
[23]   Kv, #xed, O. tek, #x159, ej, J. Siegel, V. Hnatowicz, #xed, #x160, vor, #x10d, #xed, V. k, #xe1, clav, *Journal of Nanomaterials* **2013**, *2013*, 15.

[24]   S. Kempahanumakkagari, A. Deep, K.-H. Kim, S. K. Kailasa, H.-O. Yoon, *Biosensors and Bioelectronics* **2017**, *95*, 106-116.

[25]   R. Hua, N. Hao, J. Lu, J. Qian, Q. Liu, H. Li, K. Wang, *Biosensors & bioelectronics* **2018**, *106*, 57-63.

[26]   aK. Ariga, K. Minami, L. K. Shrestha, *Analyst* **2016**, *141*, 2629-2638; bN. A. Travlou, M. Seredych, E. Rodríguez-Castellón, T. J. Bandosz, *Journal of Materials Chemistry A* **2015**, *3*, 3821-3831.

[27]   aG. Darabdhara, B. Sharma, M. R. Das, R. Boukherroub, S. Szunerits, *Sensors and Actuators B: Chemical* **2017**, *238*, 842-851; bJ. Lv, C. Kong, Y. Xu, Z. Yang, X. Zhang, S. Yang, G. Meng, J. Bi, J. Li, S. Yang, *Sensors and Actuators B: Chemical* **2017**, *248*, 630-638.

[28]   aJ. Lei, R. Qian, P. Ling, L. Cui, H. Ju, *TrAC Trends in Analytical Chemistry* **2014**, *58*, 71-78; bJ. N. Tiwari, V. Vij, K. C. Kemp, K. S. Kim, *ACS nano* **2015**, *10*, 46-80; cB. L. Li, J. Wang, H. L. Zou, S. Garaj, C. T. Lim, J. Xie, N. B. Li, D. T. Leong, *Advanced Functional Materials* **2016**, *26*, 7034-7056.

[29]   aW. Zhang, P. Zhang, Z. Su, G. Wei, *Nanoscale* **2015**, *7*, 18364-18378; bM. Pumera, A. H. Loo, *TrAC Trends in Analytical Chemistry* **2014**, *61*, 49-53.

[30]   J. Qi, W. Zhang, R. Xiang, K. Liu, H.-Y. Wang, M. Chen, Y. Han, R. Cao, *Advanced Science* **2015**, *2*, 1500199.